TIFR-BC-79/3

# INCLUSIVE PRODUCTION OF $K^*(892)$ AND $\Sigma(1385)$ IN $\bar{p}p$ INTERACTIONS AT 3.6 GeV/c AND A TEST OF FACTORIZATION HYPOTHESIS

S. BANERJEE, S.N.GANGULI, P.K.MALHOTRA, R.RAGHAVAN AND K.SUDHAKAR

Tata Institute of Fundamental Research, Bombay 5

## Abstract

We present a study of the inclusive production of $K^*(892)$ and $\Sigma^{\pm}(1385)+$ cc at 3.6 GeV/c from $\bar{p}p$ interactions. The sensitivity of the exposure is 35.4 events/μb. Longitudinal and transverse momentum distributions are presented. The indirect production of $K^0_s$ from parent $K^*$ and that of $\Lambda$'s from parent $\Sigma(1385)$ are studied. The shape of the x distribution of $\Lambda$'s for $p \overset{\bar{p}}{\rightarrow} \Lambda$ are calculated from $p \overset{p}{\rightarrow} \Lambda$ and $p \overset{\pi^-}{\rightarrow} \Lambda$ and compared with the experimental distributions. The difference of antiparticle and particle production cross-section of $K^0_s$ in the central region is compared with the expectation from Mueller-Regge formalism.

## 1. Introduction

In recent years high statistics data on the inclusive and semi-inclusive resonance production in hadron-hadron interactions have started to become available and as a result the importance of indirect production of stable hadrons like pions and kaons through resonance decays has been realised. There exists a large number of such data in pp, $\pi$p and Kp interactions, but there is a lack of similar data in nucleon-antinucleon interactions [1-7]. In this paper we present a detailed study of the inclusive reactions,

$$\bar{p} + p \rightarrow K^{*\pm}(892) + \text{anything}, \quad .. (1)$$

$$\bar{p} + p \rightarrow \Sigma^{\pm}(1385) + \text{anything}, \quad .. (2)$$

$$\bar{p} + p \rightarrow \bar{\Sigma}^{\pm}(1385) + \text{anything} \quad .. (3)$$

at 3.6 GeV/c. Experimental details are presented in sect.2. Sects.3 and 4 deal with the inclusive $K^*$ and $\Sigma(1385)$ production respectively. Sect.5 covers the phenomenological aspects of the production of $K^0_s$ and $\Lambda$ in the central and fragmentation regions respectively.

## 2. Experimental details

The data for this analysis were obtained from an exposure of 570K pictures in the CERN 2m hydrogen bubble chamber to 3.6 GeV/c antiprotons with a sensitivity of 35.4 events/$\mu$b. This exposure yielded a total of 33046 $K^0_s$'s, 7792 $\Lambda$'s and 7519 $\bar{\Lambda}$ events within a restricted fiducial volume. Further details regarding the exposure are given in ref.[8]; the details of the inclusive production of $K^0_s$, $\Lambda$ and $\bar{\Lambda}$ are

given in ref.[9].

3. Production of $K^*(892)$

The extraction of the resonance parameters has been done by analysing the effective mass distribution of the $K^0_s\pi^\pm$ system. The effective mass distribution has been fitted using a noncoherent combination of a resonance term and a background term. The final parametrisation can be written down as

$$\frac{d\sigma}{dM} = BG(1 + \alpha_1 BW) \qquad .. (4)$$

where resonance term is represented by a relativistic Breit-Wigner BW and the background term BG is a smooth function of effective mass M.

$$BW = \frac{M_R . M . \Gamma(M)}{(M^2 - M_R^2)^2 + M_R^2 \Gamma^2(M)} \qquad .. (5)$$

where $M_R$ = central mass of the resonance,

$\Gamma(M)$ = mass dependent width

$$= \Gamma_R \, (p^*/p^*_R)^{2L+1} \, \frac{\rho(M)}{\rho(M_R)},$$

$\Gamma_R$ = central width value,

$p^*$ = momentum of the daughter particle in the parent rest frame (corresponding to mass M),

$p^*_R$ = value of $p^*$ corresponding to $M = M_R$,

L = orbital angular momentum of the decay system,

$\rho(M)$ = attenuation factor $= \frac{1}{p^{*2} + p_R^{*2}}$,

and the BG has been parametrised as

$$BG = \alpha_2 (M-M_{th})^{\alpha_3} \exp(-\alpha_4 M - \alpha_5 M^2) \quad .. (6)$$

where $M_{th} = m_k + m_\pi$ in the case of $K^*(892)$.
This parametrisation is well suited for resonances produced close to the threshold. The seven parameters to be fitted are $\alpha_1, \alpha_2, \alpha_3, \alpha_4, \alpha_5$, $M_R$ and $\Gamma_R$.

The $K^o_s\pi^\pm$ mass distributions are fitted in the range $0.64\ GeV/c^2 < M(K^o_s\pi^\pm) < 1.44\ GeV/c^2$ to obtain $K^*(892)$ cross section. Fig.1 shows a clear signal of $K^*(892)$ above the background in the $K^o_s\pi^\pm$ mode. The fit yields the following mass and width for $K^*$,

$$M_R = 0.891 \pm 0.001\ GeV/c^2$$
$$\Gamma_R = 0.058 \pm 0.002\ GeV/c^2$$

which agree reasonably well with the values quoted in the particle-data group table.

3.1 Inclusive production cross section of $K^{*\pm}$

The inclusive cross section for the production of $K^{*\pm}$ is found to be,

$$\sigma(K^{*\pm}) = \sigma(K^{*+}) + \sigma(K^{*-}) = 1.477 \pm 0.015\ mb \quad .. (7)$$

The quoted error refers to statistical uncertainty only. The parametrization of the background can introduce about 5% systematic error in the cross section. Above all there is about 5% uncertainty in the absolute normalisation. To see the goodness of the fit the $K^o_s\pi^+$ and $K^o_s\pi^-$ mass plots have been

separately fitted to extract $K^{*+}$ and $K^{*-}$ contributions. The values obtained are,

$$\sigma(K^{*+}) = 0.739 \pm 0.012 \text{ mb} \quad .. (8)$$

$$\sigma(K^{*-}) = 0.741 \pm 0.012 \text{ mb} \quad .. (9)$$

These values are in good agreement with the overall fit, eq.(7). The cross sections are corrected for the unobserved decay modes, namely $K^{\pm}\pi^{0}$ and $K^{0}_{L}\pi^{\pm}$ states.

In fig.2 is plotted the inclusive $K^{*}$ cross section as a function of momentum. It is seen that the $K^{*}$ cross section is decreasing with momentum from 0.76 GeV/c to 14.75 GeV/c. This may be due to the fact that at these momenta the production of $K^{*}$ is dominantly through annihilations mechanism and that the annihilation cross section is rapidly decreasing with energy.

In table 1 we have summarised all the available data on the inclusive ratio $K^{*\pm}/(K^{0}+\bar{K}^{0})$. It is interesting to note that this ratio is independent of the incident energy.

3.2 Topological cross-section

The production cross section of $K^{*}$ is also obtained by fitting separately the events with 2,4 and 6 charged-prongs and the result is given in table 2. This enables us to calculate the associated charge multiplicity $\langle n_{ch} \rangle$ for $K^{*}$ events. The dependence of $\langle n_{ch} \rangle$ and $\langle n_{ch} \rangle / D$, with $D = [\langle n^{2}_{ch} \rangle - \langle n_{ch} \rangle^{2}]^{\frac{1}{2}}$, on incident beam energy is shown in fig.3. The dependence is seen to be very similar to that of

the $K^o_s$ [9] namely, $\langle n_{ch} \rangle$ increases with $p_{lab}$ while $\langle n_{ch} \rangle / D$ is ≈ 2 and independent of $p_{lab}$.

3.3 Indirect production of $K^o_s$ from $K^*$ decays

There is increasing evidence that a major fraction of pions and kaons originates through decays of resonances, designated here as indirect production. From the measured production cross section of $K^{*\pm}$ it is found that (24±1)% of all $K^o_s$ originate from $K^{*\pm}$. If we assume that $K^{*o}(\bar{K}^{*o})$ production cross section is the same as that of $K^{*+}(K^{*-})$ we find that (36±1)% of $K^o_s$ originate from $K^*$ decays. This indirect production of $K^o_s$ from all $K^*$ decays is numerically same as the inclusive ratio $K^{*\pm}/(K^o+\bar{K}^o)$; the latter is listed in table 1. It is thus seen that $K^*$ decays alone can account for ≈ 35% of $K^o_s$ independent of incident beam momentum in the range 0.7 - 15 GeV/c.

3.4 Transverse momentum distribution

The transverse momentum ($p_T$) distribution of $K^*$ is obtained by separating the events in $p_T^2$ bins of $K^o_s\pi^\pm$ system and then for each bin $K^*$ cross section is obtained using the procedure described in the beginning of this section. The $K^{*+}$ and $K^{*-}$ have very similar $p_T^2$ distributions and so they have been combined to improve statistical significance. In fig.4 is shown the $d\sigma/dp_T^2$ for $K^{*\pm}$. A single exponential of the type,

$$d\sigma/dp_T^2 = A \exp(-B\ p_T^2) \qquad .. (10)$$

fit the data well with A = (5.7±0.1) mb/(GeV/c)$^2$ and B = (3.8±0.1) (GeV/c)$^{-2}$. For the sake of comparison $p_T^2$ distribution of $K_s^o$ is also plotted. The $K_s^o$ distribution, however, is not a single exponential type [9]. We have also obtained the $p_T^2$ distribution of indirectly produced $K_s^o$ (from $K^{*\pm}$ decays) and it is also shown in fig.4. The indirect $K_s^o$ distribution seems to be a bit flatter than all $K_s^o$ (and steeper than the parent $K^*$), namely a single exponential fit for $p_T^2 \leq 0.4$ (GeV/c)$^2$ yields B = (5.5±0.1) (GeV/c)$^2$ for the indirect $K_s^o$ while for the all $K_s^o$ we get B = (6.7±0.1) (GeV/c)$^{-2}$. We have summarised in table 3 the values of $\langle p_T \rangle$ for $K^{*\pm}$, indirect $K_s^o$ and for all $K_s^o$.

3.5 Rapidity distribution

The rapidity distribution, $\frac{1}{\pi} d\sigma/dy^*$, for $K^{*+}$ is shown in fig.5. The rapidity variable is defined as,

$$y^* = \frac{1}{2} \ln\{(E+p_{\parallel})/(E-p_{\parallel})\} \qquad .. (11)$$

where E and $p_{\parallel}$ are the energy and longitudinal momentum of the particle in the cm system. In the figure is also shown the $y^*$ distributions for all $K_s^o$'s and also that of indirect $K_s^o$ from $K^{*+}$ decay. The average values of $y^*$ for these distributions are: -0.20 for $K^{*+}$, -0.20 for indirect $K_s^o$ from $K^{*+}$ and 0.04 for all $K_s^o$. The negative values of $\langle y^* \rangle$ for $K^{*+}$ and indirect $K_s^o$ (which are basically $K^o$) are understandable because $K^{*+}$ is produced in the proton fragmentation region as well as in the central region. The small value of $\langle y^* \rangle$ for all

$K^o_s$ is consistent with its production being symmetric around $y^* = o$ because it is an equal admixture of $K^o$ and $\bar{K}^o$.

4. Production of $\Sigma(1385)$

The mass distributions of $\Lambda\pi^+$ + charge conjugate (cc) and $\Lambda\pi^-$ + cc are shown in fig.6. Both the distributions show a clear signal for $\Sigma(1385)$. We have checked that all the distributions from $\Lambda\pi^+$ and its cc (similarly $\Lambda\pi^-$ and its cc) are similar and hence they have been combined in obtaining various distributions. The fitting of these mass distributions is done in the same way as in sect.3 in the mass range $1.26\,GeV/c^2 < M_{\Lambda\pi^\pm} < 1.70\,GeV/c^2$. The mass, width and cross section thus obtained for $\Sigma(1385)$ are summarised in table 4. The quoted cross sections are corrected for the unobserved decay mode ($\Sigma\pi$ final state and neutral decay mode of $\Lambda$).

The variation of cross section with $p_{lab}$ is shown in fig.2; the rapid increase in cross section at these energies may be due to the threshold effect.

The indirect production of $\Lambda$ from $\Sigma^\pm(1385)$ decay is found to be $(8.8\pm0.3)\%$ and similarly $\bar{\Lambda}$ from $\bar{\Sigma}^\pm(1385)$ is $(12.0\pm0.5)\%$. We have summarised in table 1 the available data regarding the indirect production of $\Lambda$ and this is seen to be increasing rapidly with momenta upto 14.75 GeV/c.

4.1 Transverse momentum distributions

The transverse momentum distributions for $\Sigma^\pm(1385)$ are obtained in a manner similar to that of the $K^*$. In fig.7 is

shown $d\sigma/dp_T^2$ distributions for $\Sigma^{\pm}(1385)$ along with that of inclusive $\Lambda$. A single exponential fit of the type $d\sigma/dp_T^2 = A \exp(-Bp_T^2)$ yielded a slope of $B = 4.3\pm0.2$ $(GeV/c)^{-2}$ for the $\Sigma^+(1385)$ and of $B = 4.7\pm0.2$ $(GeV/c)^{-2}$ for the $\Sigma^-(1385)$. In the case of inclusive $\Lambda$ the data is best fitted by a sum of two exponentials [9] with slopes as $12.18\pm0.02$ and $4.97\pm0.01$ $(GeV/c)^{-2}$; the latter slope is closer to that of $\Sigma(1385)$. We have summarised in table 3 the average $p_T$ value for $\Sigma^{\pm}(1385)$, $\Lambda$'s from $\Sigma(1385)$ and for all inclusive $\Lambda$.

4.2 Rapidity distributions

In fig.8 is shown the rapidity distributions, $\frac{1}{\pi}d\sigma/dy^*$, of $\Sigma^{\pm}(1385)$. We have also shown indirect $\Lambda$'s from $\Sigma^{\pm}(1385)$ along with all inclusive $\Lambda$'s. It is seen that $\Sigma^+(1385)$'s have the characteristic of fragments from proton like that of $\Lambda$'s, while $\Sigma^-(1385)$'s as expected have the characteristic of particles produced in the central region. The characteristics of indirect $\Lambda$'s seen to be different from those of all inclusive $\Lambda$'s.

5. Test of Factorization hypothesis

Factorization of Regge residues in conjunction with the exoticity criterion of $ab\bar{c}$ in the fragmentation process $b \xrightarrow{a} c$ enables us to relate reactions with varying incident particle 'a'; see for example ref.[11]. Several experimental tests have been made, see for example ref. [12,13], and it is found that factorization hypothesis works reasonably well in the fragmenta-

tion region. In Sect.5.1, we test factorization hypothesis by comparing the experimental x distributions of $p \overset{\bar{p}}{\to} \Lambda$ with the predicted ones from $p \overset{p}{\to} \Lambda$ and $p \overset{\pi^-}{\to} \Lambda$.

In the Mueller-Regge formalism there are three leading terms in the central region arising due to Pomeron-Pomeron (no energy dependence), Pomeron-Reggeon (energy dependence of $s^{-\frac{1}{4}}$) and Reggeon-Reggeon (energy dependence of $s^{-\frac{1}{2}}$); we have assumed the intercepts for Pomeron and Reggeon as 1 and $\frac{1}{2}$ respectively. Here s stands for square of cm energy. The Pomeron-Pomeron term will drop out if we take the difference of antiparticle and particle cross sections, $\Delta^c = (\bar{a}b \to cx) - (ab \to cx)$. Similarly, if we define $\Delta^{\bar{c}} = (\bar{a}b \to \bar{c}x) - (ab \to \bar{c}x)$ for the production of $\bar{c}$, it has been shown [14] that by taking a sum of $\Delta^c$ and $\Delta^{\bar{c}}$ we are left out with only the Reggeon-Reggeon term, i.e.,

$$\Delta^c + \Delta^{\bar{c}} \propto s^{-\frac{1}{2}} \qquad .. (12)$$

Since $K^o_s$ is an equal mixture of $K^o$ and $\bar{K}^o$, the difference of antiparticle and particle cross sections for the production of $K^o_s$ in the central region is expected to show $s^{-\frac{1}{2}}$ energy dependence; this is discussed in sect.5.2.

5.1 Λ in the fragmentation region

The following expressions can be written for the invariant cross sections in the fragmentation process $p \overset{a}{\to} \Lambda$ :

$$f(p \overset{p}{\to} \Lambda) = {}^{p}_{p}R \cdot {}^{p}_{p}P \qquad .. (13)$$

$$f^{s}(p \overset{\bar{p}}{\to} \Lambda) = \gamma^{P}_{p\bar{\Lambda}} \cdot \beta^{P}_{p} + 2\gamma^{M}_{p\bar{\Lambda}} \cdot [\beta^{f}_{p} + \beta^{\rho}_{p}] \cdot s^{-\frac{1}{2}} \quad .. (14)$$

$$f^{s}1(p \overset{\pi^-}{\to} \Lambda) = \gamma^{P}_{p\bar{\Lambda}} \cdot \beta^{P}_{\pi} + 2\gamma^{M}_{p\bar{\Lambda}} \cdot \beta_{\pi} \cdot s_1^{-\frac{1}{2}} \quad .. (15)$$

where $\beta^{i}_{a}$ is the coupling of the trajectory i to the particle 'a' and $\gamma^{i}_{b\bar{c}}$ describes it coupling to the $b\bar{c}$ system; M stands for f, $A_2$, $\rho$ or $\omega$. From the exoticity condition it can be shown [11] that the coupling of all the meson trajectories to $p\bar{\Lambda}$ system are equal and hence denoted by $\gamma^{M}_{p\bar{\Lambda}}$ and similarly from the absence of exotic exchanges in $\pi^+ \pi^+$ scattering it can be shown that $\rho$ and f coupling to $\pi$ is equal and hence denoted by $\beta_\pi$. From $\rho, \omega$ universality we can also write $\beta^{f}_{p} = 3/2\ \beta_\pi$ and $\beta^{\rho}_{p} = 1/2\ \beta_\pi$. Thus we obtain the following relation,

$$f^{s}(p \overset{\bar{p}}{\to} \Lambda) = [1-2(\beta^{P}_{\pi}/\beta^{P}_{p})(s/s_1)^{-\frac{1}{2}}]\ f(p \overset{p}{\to} \Lambda) + 2(s/s_1)^{-\frac{1}{2}}$$

$$f^{s}1(p \overset{\pi^-}{\to} \Lambda) \quad .. (16)$$

The ratio $\beta^{P}_{\pi}/\beta^{P}_{p}$ can be replaced by $\sigma^{\infty}_{tot}(\pi p)/\sigma^{\infty}_{tot}(pp)$ which we take as 0.62.

Besides our present work at 3.6 GeV/c the experimental data on $p \overset{\bar{p}}{\to} \Lambda$ exist at 4.6[15], 5.7[16], 9.1[15], 12[17], 22.4[13], 32[18] and 100[19] GeV/c. For the $p \overset{\pi^-}{\to} \Lambda$ we use 18.5 GeV/c data [20]. For the $p \overset{p}{\to} \Lambda$: we use 12 GeV/c data [21] for the first five data sets of $\bar{p}$, 24 GeV/c data [21] for the next three data sets of $\bar{p}$ and 102 GeV/c data [22] for the last 100 GeV/c $\bar{p}$ set; this way we shall take care of the small

energy dependence seen experimentally in $p \xrightarrow{p} \Lambda$. The results are presented in fig.9.

It is seen from fig.9 that the factorization prediction is very good for $\bar{p}$ data with $p_{lab} > 9$ GeV/c. For the three low momentum data sets, (3.6, 4.6 and 5.7 GeV/c) the predicted values are always more than the experimental values. This can be understood on the basis of the phase space limitation for the production of $\Lambda$ at these low momenta.

5.2 $K^o_s$ in the central region

We define the central region of $K^o_s$ as $-0.1 < x < 0.1$ with x as $p^*_{\parallel}/p^*_{max}$. From the invariant x distribution, denoted by $f(x) = (E/\pi p_{max})d\sigma/dx$, we have calculated the central region cross section through $\int_{-0.1}^{+0.1} f(x)dx$. This has been done for all the existing data [23] for ap and $\bar{a}p$ with $a = \pi$, K and p. For a given $p_{lab}$ of $\bar{a}p \to K^o_s X$ data, the corresponding values of $\int_{-0.1}^{+0.1} f(x)dx$ for $ap \to K^o_s X$ was estimated by plotting the cross sections as a function of $s^{-\frac{1}{2}}$ and interpolating between the data in the neighbourhood of $p_{lab}$. In this way we are able to calculate,

$$\Delta\sigma^a(K^o_s) = \int_{-0.1}^{+0.1} f(x)dx\Big|_{\bar{a}p} - \int_{-0.1}^{+0.1} f(x)dx\Big|_{ap} \quad ..(17)$$

In fig.10 is plotted $\Delta\sigma^a(K^o_s)$ as a function of $s^{-\frac{1}{2}}$. The dashed lines are drawn to guide the eye. The data points for $\Delta\sigma^p(K^o_s)$ cover a wide range in momentum, namely 3.6 GeV/c to 100 GeV/c, and they are in reasonable agreement with linearity in $s^{-\frac{1}{2}}$

as expected, see eq.(12).

## 6. Conclusions

The conclusions drawn from this study are as follows:

(i) The inclusive production cross sections for $K^*(892)$ and $\Sigma(1385)$ are,

$$\sigma(K^{*+}) = \sigma(K^{*-}) = 0.74\pm0.01 \text{ mb}$$
$$\sigma(\Sigma^{+}_{1385}+cc) = 70.5\pm2.0 \ \mu b$$
$$\sigma(\Sigma^{-}_{1385}+cc) = 36.4\pm1.5 \ \mu b$$

(ii) The inclusive ratio $K^{*\pm}/(K^{o}+\bar{K}^{o})$ seems to be independent of incident antiproton momentum. Nearly 35% of $K^{o}_{s}$ are produced indirectly from $K^*$ decays.

(iii) The proportion of indirect production of $\Lambda$ from $\Sigma^{\pm}(1385)$ decay seems to increase with the incident momentum. This could be attributed to the threshold effect in $\Sigma^{\pm}(1385)$ production.

(iv) The $p_T^2$ distribution of $K^*$ is flatter compared to the inclusive $K^{o}_{s}$ for $p_T^2 < 0.4$ $(GeV/c)^2$. The $p_T^2$ distribution of the indirect $K^{o}_{s}$ is also steeper than the parent $K^*$, and its slope is closer to that of the all inclusive $K^{o}_{s}$ for $p_T^2 < 0.4$ $(GeV/c)^2$.

(v) The $p_T^2$ distribution of $\Sigma^{+}(1385)$ is flatter compared to the inclusive $\Lambda$'s for $p_T^2 < 0.4$ $(GeV/c)^2$.

(vi) From the rapidity distributions of $K^*$ and $\Sigma^{\pm}(1385)$, it is concluded that $K^*$ and $\Sigma^{-}(1385)$ are dominantly

produced in the central region, while $\Sigma^+(1385)$ has a strong contribution from fragmentation of the proton.

(vii) We have made a study of factorization hypothesis from $\Lambda$'s produced in the proton fragmentation region and $K^o_s$ from the central region. The shape of the x distribution of $\Lambda$'s from $p \xrightarrow{\bar{p}} \Lambda$ can be reproduced from $p \xrightarrow{p} \Lambda$ and $p \xrightarrow{\pi^-} \Lambda$ for $\bar{p}$ momentum > 9 GeV/c. The difference of antiparticle and particle production cross section of $K^o_s$ in the central region is in reasonable agreement with $s^{-\frac{1}{2}}$ dependence as expected in the Mueller-Regge formalism.

Acknowledgements

We are grateful to Drs. B.R. French, J. Moebels and C. Pols for allowing us to use the 3.6 GeV/c $\bar{p}p$ DST.

[23] Data on $K^o_s$ from pp interactions were obtained from:
V. Blobel et al., ref.[21];
K. Jaeger et al., Phys. Rev. D11 (1975)1756, 2405;
H. Boggild et al., Nucl. Phys. B57 (1973)77;
V. Ammosov et al., Nucl. Phys. B115 (1976)269;
J.W. Chapman et al., ref.[22];
A. Sheng et al., Phys. Rev. D11 (1975)1733.
Data on $K^o_s$ from $\bar{p}p$ interactions were obtained from refs.[2,9,13,15,17,18,19].
Data on $K^o_s$ from $K^+p$ interactions were obtained from:
P.V. Chliapnikov et al., Nucl. Phys. B97 (1975)1;
B133 (1978)93;
Data on $K^o_s$ from $K^-p$ interactions were obtained from:
A. Borg et al., Nuov. Cim. 22A (1974)559;
P. Bosetti et al., Nucl. Phys. B60 (1973)307;
P. Beilliere et al., Nucl. Phys. B90 (1975)20.
Data on $K^o_s$ from $\pi^+p$ interactions were obtained from:
D.J. Crennell et al., Phys. Rev. Lett. 28 (1972)643;
P. Bosetti et al., Nucl. Phys. B94 (1975)21;
P.H. Stuntebeck et al., ref.[20].
Data on $K^o_s$ from $\pi^-p$ interactions were obtained from:
F. Barreiro et al., Phys. Rev. D17 (1978)669;
P.H. Stuntebeck et al., ref.[20];
D. Ljung et al., Phys. Rev. D15 (1977)3163.
D. Bogert et al., Phys. Rev. D16 (1977)2098.

## References


[1] R.Hamatsu et al., Nucl. Phys. B123 (1977)189.

[2] A.M.Cooper et al., Nucl. Phys. B136 (1978)365.

[3] P.Gregory et al., Nucl. Phys. B119 (1977)60.

[4] J.F.Baland et al., Nucl. Phys. B140 (1978)220.

[5] J. Canter et al., paper presented at the IVth European Antiproton Symposium held at Barr/Strasbourg (1978).

[6] D.I. Ermilova et al., Nucl. Phys. B137 (1978)29.

[7] R. Raja et al., Phys. Rev. D16 (1977)2733.

[8] H.W. Atherton et al., Nucl. Phys. B69 (1974)1;
B.R. French et al., Nucl. Phys. B119 (1977)237.

[9] S. Banerjee et al., Nucl. Phys. B150 (1979)119.

[10] H. Muirhead, private communication (1979).

[11] H.I. Miettinen, Phys. Lett. 38B (1972)431.

[12] P. Gregory et al., Nucl. Phys. B122 (1977)435.

[13] E.G. Boos et al., paper submitted to the International Conference on High Energy Physics, Tokyo, 1978.

[14] J.G. Rushbrooke and B.R. Webber, Phys. Reports 44 (1978)1.

[15] M.T. Regan et al., Nucl. Phys. B141 (1978)65.

[16] S.N. Ganguli and B. Sadoulet, Nucl. Phys. B53 (1973)458.

[17] D.R. Bertrand et al., Nucl. Phys. B128 (1977)365.

[18] M.A. Jabiol et al., Nucl. Phys. B127 (1977)365.

[19] R. Raja et al., Phys. Rev. D15 (1977)627.

[20] P.H. Stuntebeck et al., Phys. Rev. D9 (1974)608.

[21] V. Blobel et al., Nucl. Phys. B69 (1974)454.

[22] J.W. Chapman et al., Phys. Lett. 47B (1973)465.

Table Captions

1. Fractions of indirectly produced $K^0_s$ and from $K^*$ and $\Sigma^\pm$ decays in $\bar{p}p$ interactions.

2. Cross sections of $K^{*+}$ and $K^{*-}$ in $\bar{p}p$ interactions at 3.6 GeV/c.

3. Average $p_T$ values (in GeV/c) of inclusively produced $K^*(892)$, $K^0_s$, indirectly produced $K^0_s$, inclusively produced $\Sigma^\pm(1385)$, $\Lambda$ and indirectly produced $\Lambda$.

4. Mass, width and cross sections of inclusively produced $\Sigma^+(1385)$ and $\Sigma^-(1385)$.

Table 1

| $P_{lab}$ (GeV/c) | $K^{*\pm}/(K^{o}+\bar{K}^{o})$ | $\Lambda$ (from $\Sigma^{\pm}(1385)$)/$\Lambda$(all) |
|---|---|---|
| 0.76 [2] | 0.36 ± 0.01 | - |
| 3.6 | 0.36 ± 0.01 | 0.088 ± 0.003 |
| 12.0 [4] | 0.23 ± 0.05 | 0.165 ± 0.030 |
| 12.0 [10] | 0.32 ± 0.08 | - |
| 14.75 [5] | 0.31 ± 0.03 | 0.23 ± 0.02 |

Table 2

| No. of prongs | $\sigma(\bar{p}p \to K^{*+} X)$ μb | $\sigma(\bar{p}p \to K^{*-} X)$ μb |
|---|---|---|
| 2 | 353.7 ± 7.9 | 369.5 ± 8.1 |
| 4 | 374.2 ± 8.1 | 359.3 ± 8.0 |
| 6 | 11.9 ± 1.4 | 12.5 ± 1.5 |
| Total | 739.1 ±11.6 | 741.3 ±11.6 |

Table 3

| Beam momentum GeV/c | Average $p_T$ values in GeV/c for | | | | | | |
|---|---|---|---|---|---|---|---|
| | $K^{*\pm}$ | $K^0_s$ (all) | Indirect $K^0_s$ | $\Sigma^+ + cc$ | $\Sigma^- + cc$ | $\Lambda$ (all) | Indirect $\Lambda$ |
| 0.76 | 0.343 ± 0.010 | 0.309 ± 0.006 | 0.313 ± 0.009 | | | | |
| 3.6 | 0.446 ± 0.002 | 0.364 ± 0.001 | 0.376 ± 0.002 | 0.389 ± 0.006 | 0.354 ± 0.007 | 0.345 ± 0.002 | 0.350 ± 0.004 |

Table 4

| Final state | Mass(GeV/$c^2$) | Width(GeV/$c^2$) | Cross-section(μb) |
|---|---|---|---|
| $\Sigma^+(1385)+cc$ | 1.383±0.001 | 0.035±0.002 | 70.5±2.0 |
| $\Sigma^-(1385)+cc$ | 1.388±0.002 | 0.036±0.004 | 36.4±1.5 |

Figure Captions

1. Effective mass distribution of $K^0_s\pi^\pm$. The solid line shows the fit to this mass distribution.

2. Inclusive cross section of $\bar{p}p \to K^*(892)^\pm$, $\bar{p}p \to \Sigma(1385)^+ + cc$, $\bar{p}p \to \Sigma^-(1385) + cc$ as a function of incident beam momentum.

3. a) Mean associated charged multiplicity $\langle n_{ch} \rangle$ as a function of beam momentum for $K^0_s$ and $K^{*\pm}$ production.
   b) Ratio of mean associated charged multiplicity to dispersion $\langle n_{ch} \rangle / D$ as a function of incident beam momentum.

4. $p_T^2$ distribution for inclusive production of $K^{*\pm}$ and $K^0_s$ and also for $K^0_s$'s produced indirectly from $K^{*\pm}$ decay. The solid and dashed lines are exponential fits $[\frac{d\sigma}{dp_T^2} = A \exp(-B\, p_T^2)]$ to these distributions.

5. Invariant cross section, $f(y^*) = \frac{1}{\pi} \int \frac{d\sigma}{dp_T^2 dy^*} dp_T^2$, as a function of cm rapidity variable $y^*$ for inclusive $K^{*+}$ and $K^0_s$ and also for $K^0_s$'s coming indirectly from $K^{*+}$ decay.

6. a) Effective mass distribution of $\Lambda\pi^-$ and its charge conjugate state. The solid line shows a fit to this distribution.
   b) The same for $\Lambda\pi^+$ and its charge conjugate state.

7. $p_T^2$ distribution for inclusive production of $\Sigma^+(1385)(+cc)$, $\Sigma^-(1385)(+cc)$ and also for $\Lambda$'s coming indirectly through

$\Sigma^{\pm}(1385)$ decays. The solid lines are exponential fits to these distributions [$\frac{d\sigma}{dp_T^2} = A \exp(-bp_T^2)$].

8. Invariant cross section, $f(y)_{lab}$, as a function of rapidity $y_{lab}$ in the target rest frame, for inclusive $\Sigma^{+}(1385)(+cc)$, $\Sigma^{-}(1385)(+cc)$, $\Lambda$ and also for $\Lambda$'s coming from $\Sigma^{\pm}(1385)$ decays.

9. Invariant cross section, $f(x) = \frac{1}{\pi p^{max}} \int \frac{d^2\sigma}{dx dp_T^2} dp_T^2$, as a function of x for the reaction $\bar{p}p \to \Lambda X$ at momenta of 3.6, 4.6, 5.7, 9.1, 12.0, 22.4, 32 and 100 GeV/c. Predictions to this cross section in the fragmentation region from the reactions $\pi^- p \to \Lambda X$ and $pp \to \Lambda X$ are also shown in the figure.

10. The difference of $K_s^o$ production in the central region in antiparticle and particle reactions, $\Delta\sigma^a = \int_{-0.1}^{0.1} f(x)dx|_{\bar{a}p} - \int_{-0.1}^{0.1} f(x)dx|_{ap}$ as a function of $s^{-\frac{1}{2}}$ (s being the square of cm energy). Points have been plotted with a = $\pi$, k, p. The dashed lines are shown to guide the eyes.

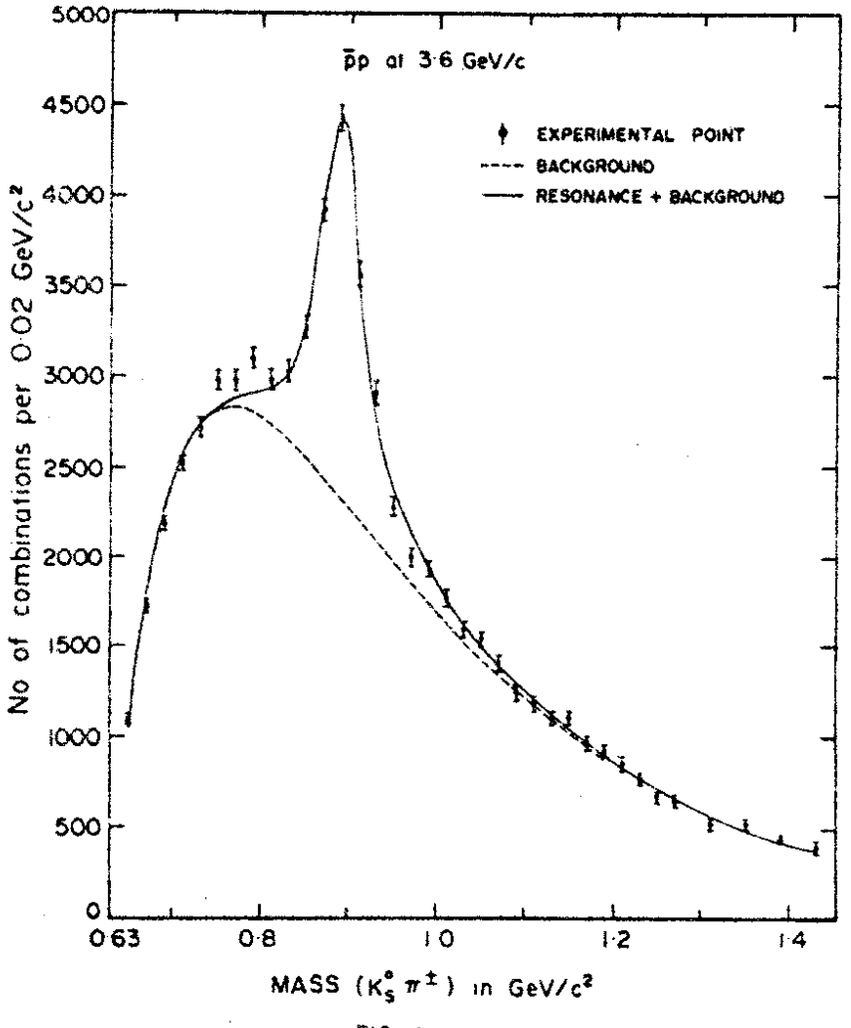
p̄p at 3·6 GeV/c
EXPERIMENTAL POINT
BACKGROUND
RESONANCE + BACKGROUND
No of combinations per 0·02 GeV/c²
MASS ($K^0_S \pi^\pm$) in GeV/c²
5000
4500
4000
3500
3000
2500
2000
1500
1000
500
0
0·63
0·8
1·0
1·2
1·4

FIG 1

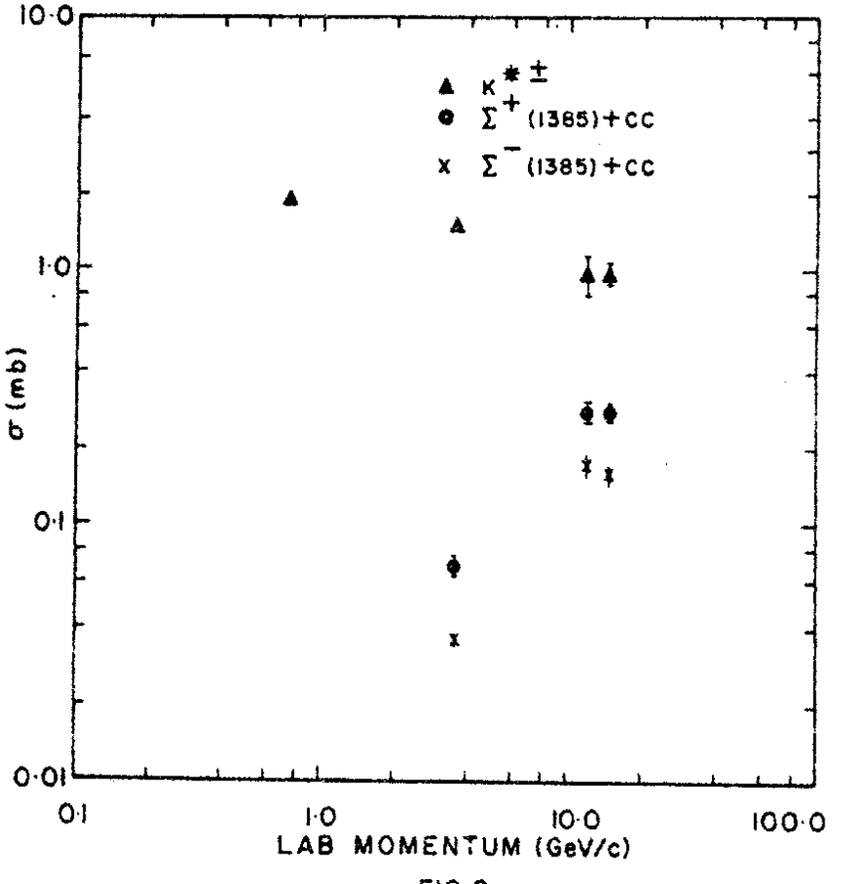
$K^{*\pm}$
$\Sigma^+(1385)+cc$
$\Sigma^-(1385)+cc$
σ (mb)
LAB MOMENTUM (GeV/c)
10·0
1·0
0·1
0·01
0·1
1·0
10·0
100·0

FIG.2

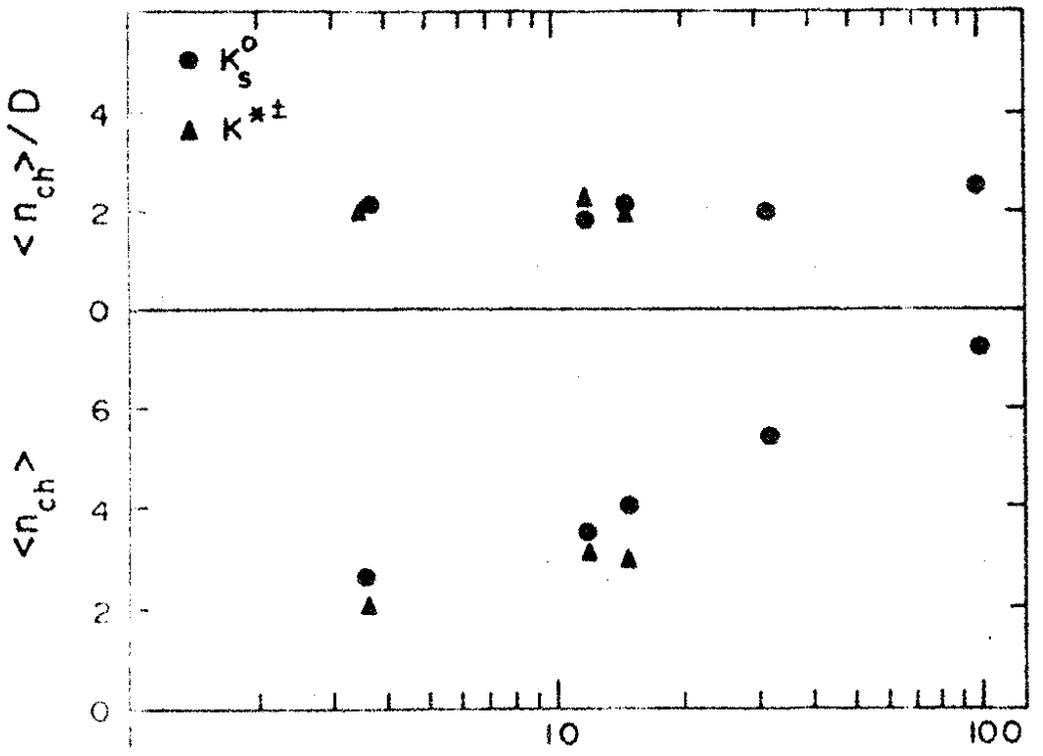
$K_s^0$
$K^{*\pm}$
$\langle n_{ch} \rangle / D$
$\langle n_{ch} \rangle$
0
2
4
6
10
100
LAB MOMENTUM (GeV/c)

FIG. 3

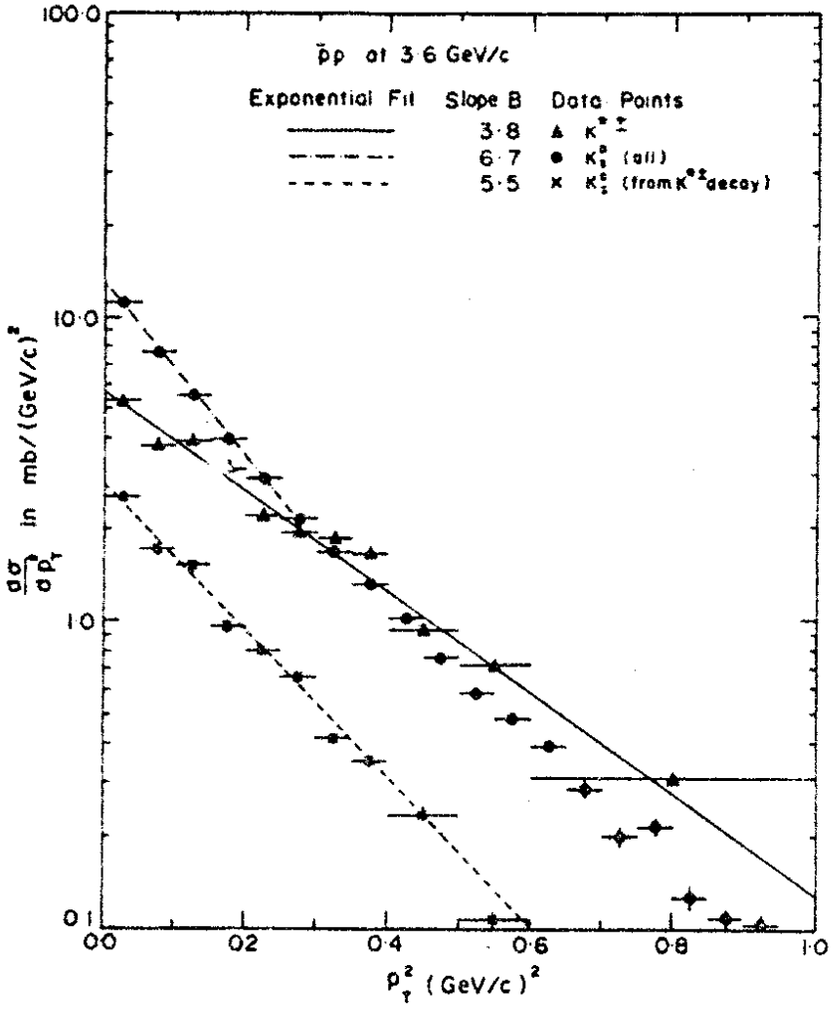
p̄p at 3·6 GeV/c
Exponential Fit
Slope B
Data Points
3·8
6·7
5·5
$K^{*\pm}$
$K^0_s$ (all)
$K^0_s$ (from $K^{*\pm}$ decay)
100·0
10·0
1·0
0·1
0·0
0·2
0·4
0·6
0·8
1·0
$\frac{d\sigma}{dp_T^2}$ in mb/(GeV/c)$^2$
$p_T^2$ (GeV/c)$^2$

Fig. 4

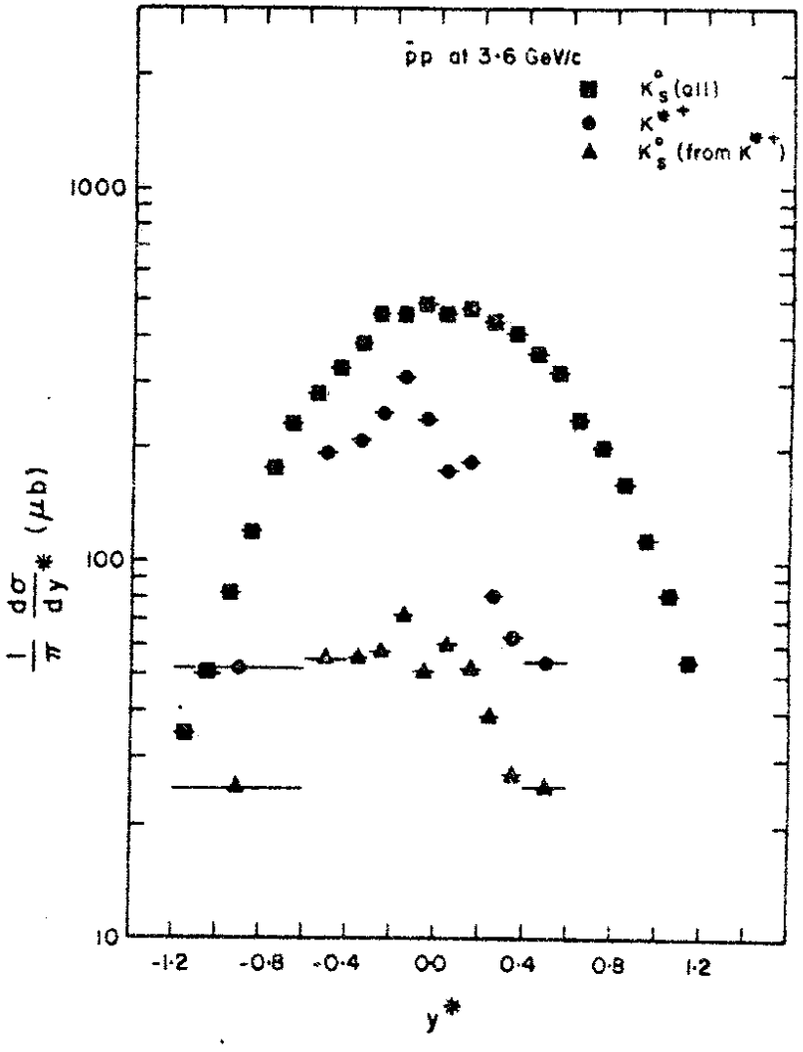
p̄p at 3·6 GeV/c
$K^0_s$ (all)
$K^{*+}$
$K^0_s$ (from $K^{*+}$)
1000
100
10
-1·2
-0·8
-0·4
0·0
0·4
0·8
1·2
$\frac{1}{\pi}\frac{d\sigma}{dy^*}$ (μb)
$y^*$

FIG. 5

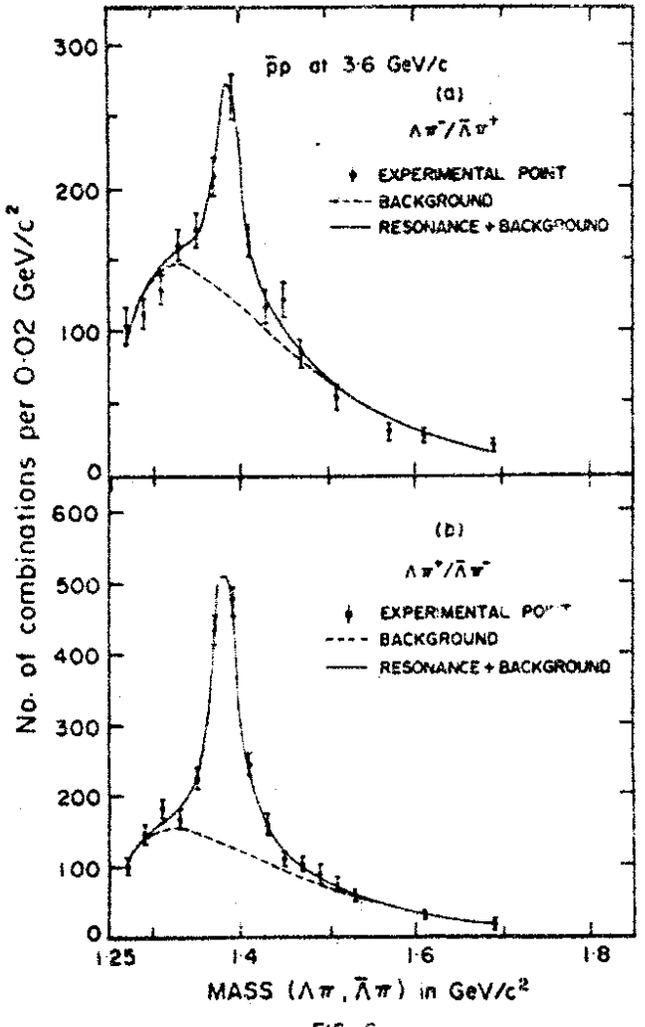
p̄p at 3·6 GeV/c
(a)
Λπ⁻/Λ̄π⁺
EXPERIMENTAL POINT
BACKGROUND
RESONANCE + BACKGROUND
(b)
Λπ⁺/Λ̄π⁻
EXPERIMENTAL POINT
BACKGROUND
RESONANCE + BACKGROUND
No. of combinations per 0·02 GeV/c²
MASS (Λπ, Λ̄π) in GeV/c²
300
200
100
0
600
500
400
300
200
100
0
1·25
1·4
1·6
1·8

FIG 6

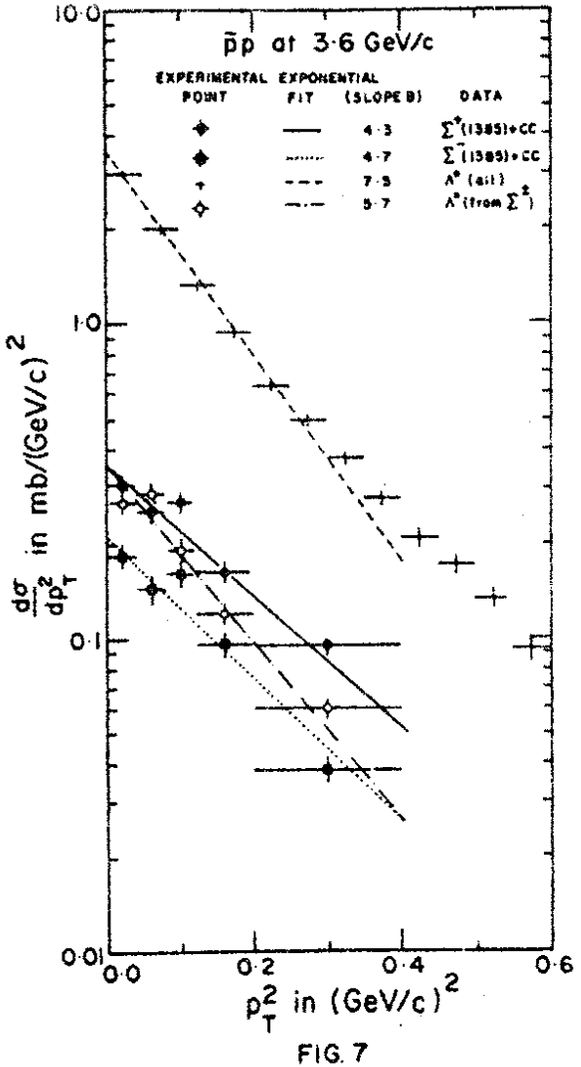
p̄p at 3·6 GeV/c
EXPERIMENTAL POINT
EXPONENTIAL FIT (SLOPE B)
DATA
4·3
Σ⁺(1385)+cc
4·7
Σ⁻(1385)+cc
7·5
Λ⁰ (all)
5·7
Λ⁰ (from Σ⁰)
dσ/dp²T in mb/(GeV/c)²
p²T in (GeV/c)²
10·0
1·0
0·1
0·01
0·0
0·2
0·4
0·6

FIG. 7

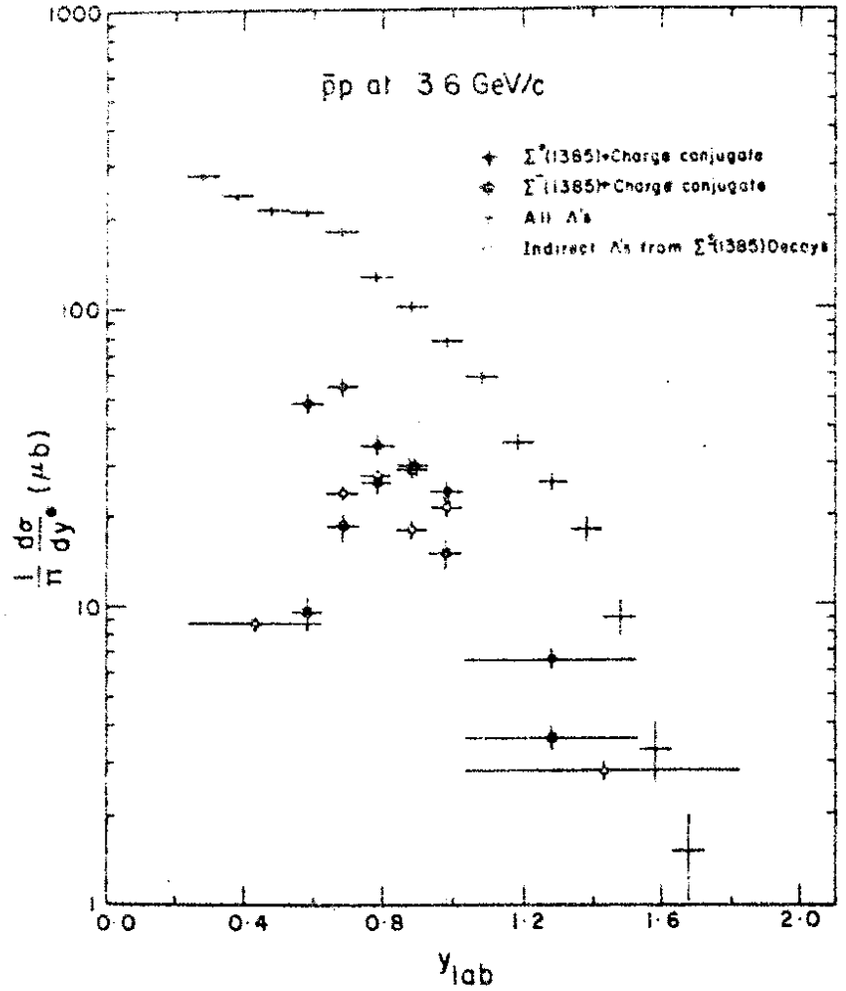
p̄p at 3 6 GeV/c
Σ°(1385)+Charge conjugate
Σ⁻(1385)+Charge conjugate
All Λ's
Indirect Λ's from Σ°(1385)Decays
1000
100
10
1
0·0
0·4
0·8
1·2
1·6
2·0
y_lab
1/π dσ/dy* (μb)

Fig 8

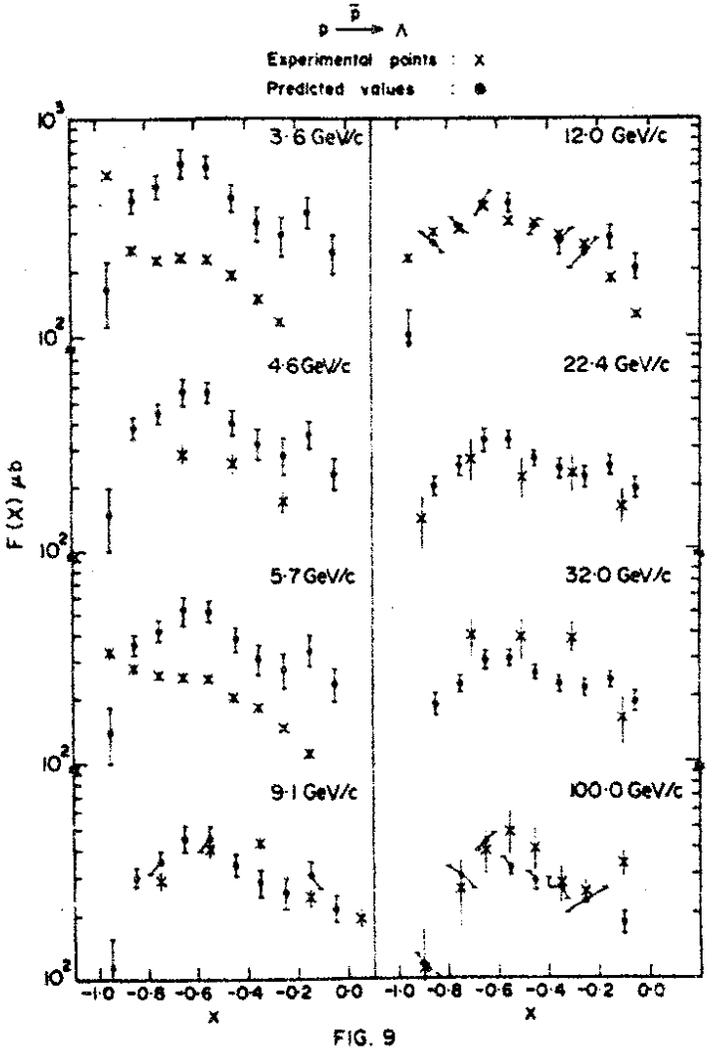
p → Λ
Experimental points : X
Predicted values : ●
3·6 GeV/c
4·6 GeV/c
5·7 GeV/c
9·1 GeV/c
12·0 GeV/c
22·4 GeV/c
32·0 GeV/c
100·0 GeV/c
F(X) μb
X

FIG. 9

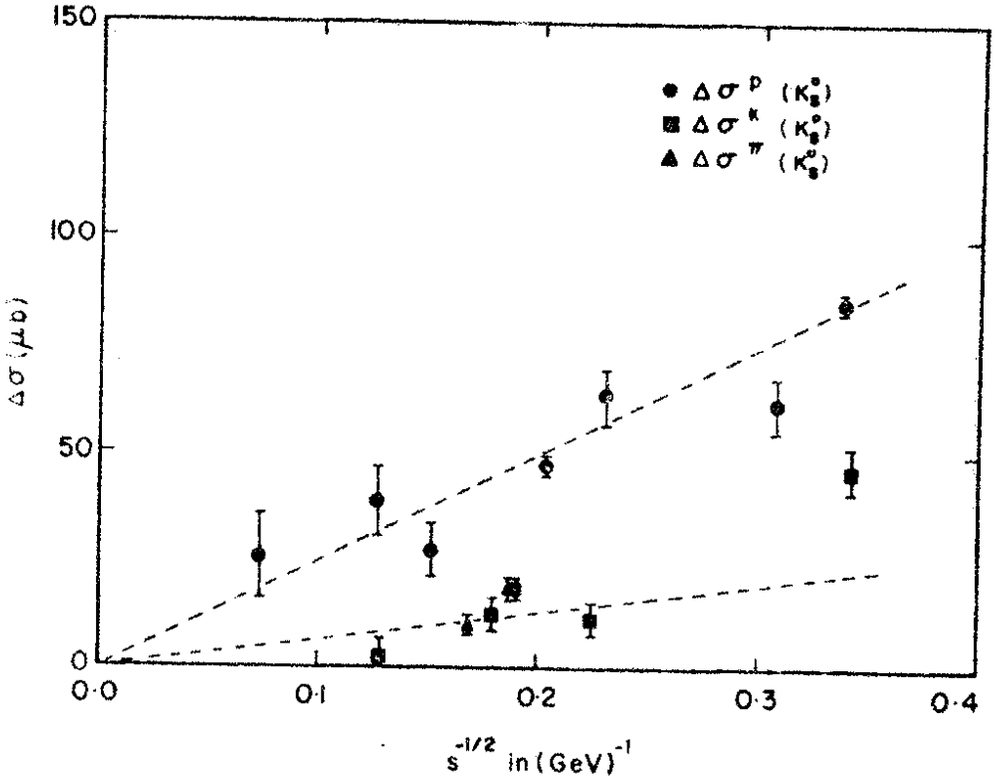


Fig. 10